

Article

Mono- and Bi-Molecular Adsorption of SF₆ Decomposition Products on Pt Doped Graphene: A First-Principles Investigation

Yongqian Wu ¹, Shaojian Song ^{1,*}, Dachang Chen ² and Xiaoxing Zhang ^{2,3}¹ School of Electrical Engineering, Guangxi University, Nanning 530004, China; fly_xideo@163.com² School of Electrical Engineering, Wuhan University, Wuhan 400044, China; chendachang@163.com (D.C.); xiaoxing.zhang@outlook.com (X.Z.)³ State Key Laboratory of Power Transmission Equipment & System Security and New Technology, Chongqing University, Chongqing 400044, China

* Correspondence: sjsong03@163.com; Tel.: +86-135-1771-9260

Received: 25 September 2018; Accepted: 19 October 2018; Published: 22 October 2018



Abstract: Based on the first-principles of density functional theory, the SF₆ decomposition products including single molecule (SO₂F₂, SOF₂, SO₂), double homogenous molecules (2SO₂F₂, 2SOF₂, 2SO₂) and double hetero molecules (SO₂ and SOF₂, SO₂ and SO₂F₂, SOF₂ and SO₂F₂) adsorbed on Pt doped graphene were discussed. The adsorption parameters, electron transfer, electronic properties and energy gap was investigated. The adsorption of SO₂, SOF₂ and SO₂F₂ on the surface of Pt-doped graphene was a strong chemisorption process. The intensity of chemical interactions between the molecule and the Pt-graphene for the above three molecules was SO₂F₂ > SOF₂ > SO₂. The change of energy gap was also studied and according to the value of energy gap, the conductivity of Pt-graphene before and after adsorbing different gas molecules can be evaluated.

Keywords: SF₆ decomposition components; Pt modified graphene; gas adsorption; density functional theory

1. Introduction

SF₆ gas has been widely used in gas insulated switch-gear (GIS) because of its excellent insulation and arc extinguishing performance but long-term operation experience shows that different degrees of partial discharge (PD) will occur in GIS equipment due to inherent defects or some new insulation problems [1–4]. With the increase of running time, these defects develop further, which may eventually lead to serious insulation problems of GIS equipment, resulting in irreparable losses. The energy produced by the discharge causes SF₆ to decompose into SF₄, SF₃, SF₂ and other low-fluorine sulfides when the discharge continues. Some of the low-fluorine sulfides react with trace amounts of water and oxygen in GIS equipment to form SO₂F₂, SOF₂, H₂S and SO₂ [5,6]. Many scholars have shown that by detecting the content of these characteristic decomposition products, the severity of insulation defects in GIS can be judged to a certain extent, and insulation accidents can be prevented. Therefore, the detection of SF₆ decomposition component content has important research significance and application value.

Graphene, a typical two-dimensional carbon nanomaterial composed of sp² hybrid orbital carbon atoms, was first discovered in 2004. Due to its excellent mechanical, electrical, optical and thermal properties, it has led extensive research in many fields such as electronics, energy, biological and chemical sensors [7–9]. In 2007, graphene was first used as a sensing material and showed selectivity for typical small molecule gases [10]. Since then, its excellent sensing performance has attracted a lot of attention. The micro gas sensor made of graphene has the advantages of low operating temperature,

high sensitivity and small size. In recent years, some scholars have made great progress in this field, using graphene as a sensitive material to detect H_2 , NH_3 , NO_2 and other gases. This provides a new idea for the detection of SF_6 decomposition products. Gas sensors based on intrinsic graphene have less response to various SF_6 decomposition products and poor recovery and selectivity. In order to improve the gas sensitivity of graphene, the preparation of graphene-based composites can significantly improve the gas sensitivity of SF_6 decomposition products, including sensitivity, response speed and recovery characteristics [11].

Nowadays, theoretical evaluation of 2D materials based on ab initial study has been widely developed. The gas sensing properties evaluated by first-principles method was an effective way to exploit high selectivity new gas sensing materials or new modified method to the surface of materials, especially for 2D graphene like materials [12,13]. To obtain the 2D material with global minimum total energy or to get the adsorption structure with the global minimum total energy rather than the local minimum, several initial structures should be considered and several optimized structures were obtained. By comparing the final total energy or other physical properties, the final structure of materials or adsorption structure can be obtained [14,15]. It has been proved that single-layer graphene without any defects has very weak chemical interactions with most of the gas molecules [16]. To enhance the interactions between the adsorbed gas molecule and the surface of graphene, introducing transition metal or noble metal was proved to be an effective way by theoretical evaluation. Doping Fe atom or Pt atom can obviously enhance the chemical interactions between single and double layered graphene with CO, NO, SO_2 and HCN [17]. Especially for Pt atom or nanoclusters, they can bring many active sites on the surface of graphene as well as provide many adsorption sites for gas molecules. As a result, the structure, electronic properties and gas adsorption behavior of Pt decorated or doped graphene has been systematically studied using quantum chemistry methods. The decoration of Pt adatom on graphene surface can apparently elevate the adsorption energy and electron transfer with not only inorganic small molecules (such as SO_2 , O_3 , NO, H_2S), but also organic molecule (such as C_2H_2 , C_2H_4 , CH_3OH and C_2H_5OH) [18–23]. Because of the excellent adsorption and gas sensing properties of Pt-graphene, in this work, we discussed the adsorption behavior of several kinds of SF_6 decomposition products on the surface of Pt doped graphene, we carried out the ab initial study with the density functional theory calculation including the adsorption energy, adsorption distance, electron transfer and electronic properties. Considering the probable appearance of several kinds of gas molecules on the surface, we further discussed the co-adsorption of two gas molecules with the same type or different type. The study can provide a guiding effect for Pt doped graphene based gas sensor used in field of detecting SF_6 decomposition products in electrical engineering.

2. Method

The adsorption of three kinds of SF_6 decomposition products (SO_2 , SOF_2 and SO_2F_2) on the surface of Pt-graphene was all carried out in Dmol³ package [24,25]. The generalized gradient approximation (GGA) with the Perdew-Burke-Ernzerhof function (PBE) was used in considering of the exchange-correlation functional [26]. The basis set chosen for this study was the double numerical plus polarization (DNP) and considering that Pt is a heavy element, the DFT semi-core pseudopotential (DSSP) was selected. To make a good description of long range vdW force, the DFT-D method was chosen force [27]. The cutoff radius for all atom in all structures was set as 5 Å. All the geometric optimizations were set of 1×10^{-5} Ha energy convergence, 0.002 Ha/Å force convergence, and 0.005 Å displacement convergence between the two iteration steps. The k-point sample of Monkhorst-Pack grid was set as $6 \times 6 \times 1$ when carrying out geometric optimization as well as the calculations of electronic properties [28]. The Gaussian smearing was 0.005 Ha.

A $6 \times 6 \times 1$ graphene supercell including 72 C atoms was first built with height of 15 Å vacuum region. To build the structure of Pt doped graphene, one C atom was substituted by one Pt atom and then the geometric optimization using the convergence criteria above. Finally, the structure of one Pt

doped graphene was obtained. For gas adsorption on the surface, one or two gas molecules were placed above the Pt atom and then the final structures were also obtained by fully geometric optimization.

The adsorption energy of one or two gas molecules on the surface of Pt-graphene is:

$$\Delta E_{ads} = E_{(molecule-Pt-graphene)} - E_{(Pt-graphene)} - E_{(molecule)} \quad (1)$$

where $E_{molecule-Pt-graphene}$, $E_{Pt-graphene}$ and $E_{molecule}$ are the calculated total energy of gas molecules/Pt-graphene adsorption structure, Pt-graphene surface before adsorption and gas molecules before adsorption. The charge transfer was based on Mulliken method [29]. The electron transfer is calculated as:

$$Q_T = Q_1 - Q_0 \quad (2)$$

where Q_1 and Q_0 represent the carried charge of adsorbed gas molecules and isolated gas molecules. The carried charge of isolated gas molecule is zero and when Q_T is negative, gas molecule obtains electrons and when Q_T is positive, gas molecule acts as electron donor.

The energy gap of the structure reflects the difficulty level of electron transition from the highest occupied molecular orbital (HOMO) to the lowest unoccupied molecular orbital (LUMO). The smaller value indicates the easier process of electron transferring from the valence band to the conduction band resulting in large conductance. The value of energy gap E_g is defined as:

$$E_g = |E_{HOMO} - E_{LUMO}| \quad (3)$$

We also calculated the density of states of adsorption structures in this study.

3. Results and Discussion

3.1. Structure of SF₆ Decomposition Products and Pt-Graphene

At the Materials Visualizer module, three kinds of SF₆ decomposition gas molecule models were constructed and after fully geometric structure optimization, three energetically stable structures were obtained. The stable structures of SO₂, SOF₂ and SO₂F₂ gas molecules are shown in Figure 1a–c the geometric parameters of these three gas molecules are listed in Table S1. The parameters obtained by this model are in good agreement with those obtained by other researchers [30].

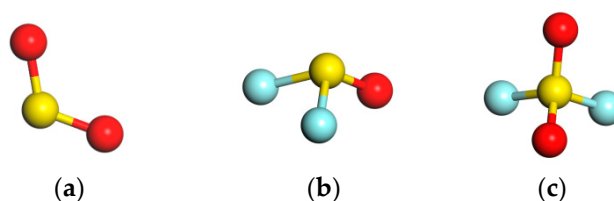


Figure 1. Geometric structures after optimization: (a) SO₂ molecule; (b) SOF₂ molecule; (c) SO₂F₂ molecule. (Yellow = Sulfur; Red = Oxygen; Cyan = Fluorine, the labels are also applied to the following figures.).

The Pt atom does not change the overall two-dimensional planar structure of graphene, but forms a local sp³ hybridization near the Pt atom and protrudes to the plane of the C atom, as shown in Figure 2. The Pt atom forms covalent bonds with three adjacent C atoms. The length of the covalent bonds of C-Pt atoms is 1.956 Å. Therefore, the formation of local sp³ configuration of Pt atoms can be further determined. Similar doping configurations have been demonstrated in graphene doped with other metal elements (Pd, Mn, Au, etc.) [31,32]. At present, there is basically a consensus that the local sp³ hybridization is the correct configuration for the theoretical study of metal doped graphene. The detailed geometric parameters of Pt-graphene are listed in Table S2.

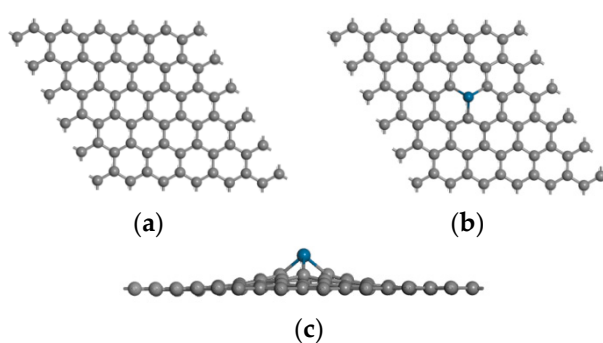


Figure 2. Geometric structures after optimization: (a) Int-graphene; (b) Top view of Pt-graphene; (c) Side view of Pt-graphene. (Grey = Carbon; Dark blue = Platinum, the labels are also applied to the following figures.).

3.2. Adsorption of Single Molecule, Double Molecules on Pt-Graphene

In this section, based on the first-principles density functional theory, the adsorption properties of SO_2 , SOF_2 and SO_2F_2 on Pt-doped graphene were studied systematically. The adsorption structure, adsorption energy and charge transfer were calculated and analyzed in detail. The modification mechanism of Pt-doped graphene and the gas-sensing response mechanism of SO_2 , SOF_2 and SO_2F_2 were evaluated. We have obtained several adsorption structures with the local minimum total energy. By comparing the adsorption energy, we only chose the structure with the maximum adsorption energy for further analysis including structure parameters and electronic properties. All the adsorption structures with the local minimum adsorption energy are shown in Figures S1–S3.

3.2.1. Analysis of Adsorption Structures and Electronic Properties

After optimizing the adsorption structures, the gas molecules were relaxed to various positions on the Pt-graphene surface. The adsorption of single and multiple gas molecules were both studied. In order to obtain the most stable adsorption structure of each gas molecule, we simulated the adsorption structure at different adsorption angles and distances. The most stable structures are shown in Figures 3–5. In order to analyze the adsorption properties, as shown in Table 1, the binding energies E_{ads} , charge transfer Q_T and adsorption distance D for different gas adsorption structures are shown. D represents the closest distance between the gas molecules and the surface of the Pt-graphene, where D_1 and D_2 represent the distances of the different gas molecules from the Pt nanoparticles, respectively. Similarly, Q_{T1} and Q_{T2} represent charge transfer between two different gas molecules and the surface, respectively. E_{ads} is the adsorption energy, and negative values indicate that the adsorption is exothermic and the reaction can occur spontaneously.

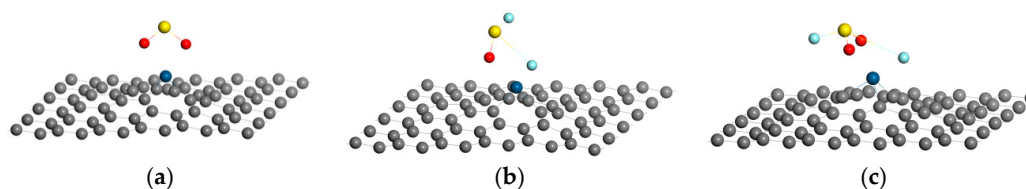


Figure 3. The adsorption structures for single SO_2 , SOF_2 and SO_2F_2 adsorption on Pt-graphene. (a) SO_2 ; (b) SOF_2 ; (c) SO_2F_2 .

The adsorption parameters and structures of single SO_2 , SOF_2 and SO_2F_2 molecules adsorbed on graphene are shown in Table 1 and Table S3 and Figure 3a–c. The O atom of SO_2 is the closest to the Pt atom. Since the electronegativity of O atom is strong, the adsorption distance is 2.261 Å. The S atom is far from the surface of Pt doped graphene because it establishes a stable covalent bond with O atom and it is difficult to interact with Pt atoms. The structure of SO_2 remains almost unchanged during

the adsorption process, and the S-O bond length of SO₂ itself is gradually extended from 1.480 Å to 1.581 Å, indicating that a new Pt-O bond may be formed during the interaction between SO₂ and Pt-doped graphene, resulting in the stretching of S-O bond of SO₂ itself. When a SOF₂ gas molecule or a SO₂F₂ molecule is close to Pt-graphene, the length of the S-F₁ bond of the adsorbed SOF₂ molecule is extended to 2.966 Å, and the length of the S-F₂ bond of the SO₂F₂ molecule is extended to 3.434 Å, indicating that the S-F bond may have been broken. According to Figure 3b,c, the broken F atom tends to form a new bond with the Pt atom. The distance between the two atoms is 2.012 Å and 2.029 Å. At the same time, the S atom tends to form a Pt-S bond with the Pt atom. In order to explore the strength of adsorption, the adsorption energies under various conditions were discussed. It can be seen from Table 1 that the adsorption of SO₂F₂ gas molecules is the strongest, because the adsorption energy is −2.429 eV. The adsorption of SO₂ on the Pt-doped graphene surface is lower than that of the SO₂F₂. The adsorption of SOF₂ and Pt doped graphene is the weakest because the adsorption energy is −1.254 eV. The charge transfer quantities of SO₂, SOF₂ and SO₂F₂ molecules with Pt-doped graphene surface as shown in Table 1 are −0.412 *e*, −0.679 *e* and −0.981 *e*. The charge transfer quantities *Q* in all three cases are negative. It is shown that electrons transfer from Pt doped graphene surface to gas molecule during the adsorption process. The gas molecules SO₂F₂, SO₂ and SOF₂ all show the characteristics of electron acceptor.

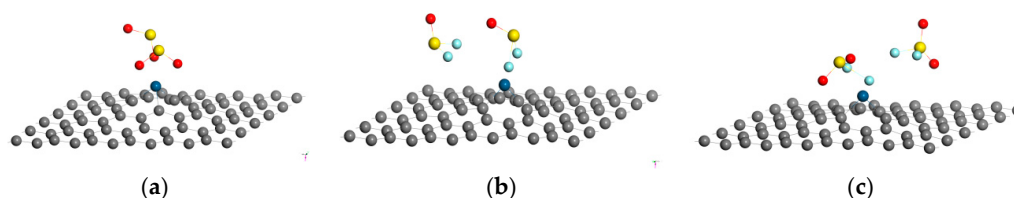


Figure 4. The adsorption structures for double SO₂, SOF₂ and SO₂F₂ adsorption on Pt-graphene. (a) 2SO₂; (b) 2SOF₂; (c) 2SO₂F₂.

The adsorption results for double gas molecules are shown in Table 1 and Table S4 and Figure 4a–c. Similar to the adsorption of a single SO₂ molecule, the SO bond length in two SO₂ gas molecules is extended from 1.480 Å to 1.498 Å (O₁-S), 1.561 Å (O₂-S), 1.565 Å (O₃-S), 1.561 Å (O₄-S). Referring to Figure 4, the interaction between the Pt-doped graphene and the double-SO₂ gas molecules may respectively form a new Pt-O bond, which leads to the stretching of the S-O bond of SO₂. During the adsorption of double SOF₂ molecules, the bond length of one SOF₂ gas molecule is unchanged, while the S-F bond length of another SOF₂ molecule is extended to 3.027 (S-F₁), 1.801 (S-F₂). This indicates that an S-F bond has broken during the adsorption process. It is also shown that only one SOF₂ gas molecule in the double SOF₂ gas molecule interacts with the surface of Pt-doped graphene, and the adsorption distances are 2.008 Å and 3.806 Å, respectively. Similarly, according to SO₂F₂ adsorption, one SO₂F₂ molecule is deformed into one SO₂ and two fluorine atoms are adsorbed on the Pt atom, and the S-F bond length is extended to 2.343 (S-F₁), 3.384 (S-F₂). The bond length of another SO₂F₂ gas molecule is unchanged, and the adsorption distance from the Pt atom is 3.422 Å. That is to say, Pt doped graphene adsorbs one of the double SO₂F₂ molecules on the surface, and the two S-F bonds were broken during the adsorption process. It can be seen from Table 1 that the adsorption energies of two-gas molecules 2SO₂, 2SOF₂, 2SO₂F₂ and Pt-doped graphene are −2.223 eV, −0.934 eV and −2.159 eV, respectively. Compared with adsorbing a single gas molecule, the adsorption properties of two gas molecules have not changed, and both belong to chemical adsorption. Since a Pt atomic site can interact with two SO₂ gas molecules, the adsorption energy is increased and nearly doubled. Charge transfer *Q_T* of 2SO₂, 2SOF₂, 2SO₂F₂ with Pt doped graphene surfaces are −0.665 *e*, −0.662 *e* and −1.088 *e*, respectively. Similar to the charge transfer amount of single molecule adsorption, the charge transfer amount *Q_T* of all three cases is negative. It indicates that during the adsorption process, electrons are transferred from the Pt-doped graphene surface to the gas molecules, and the gas molecules SO₂, SOF₂ and SO₂F₂ shows the characteristics of the electron acceptor.

Table 1. Adsorption energy (E_{ads}), charge transfer (Q_T) and binding distance (D) from adsorbed gas molecules to Pt-graphene.

System	E_{ads} (eV)	Q_{T1} (eV)	Q_{T2} (eV)	D_1 (Å)	D_2 (Å)	Bond Length (Å)
SO ₂	−1.358	−0.412		2.261		1.581 (O ₁ -S), 1.582 (O ₂ -S)
SOF ₂	−1.254	−0.679		2.012		2.966 (S-F ₁), 1.688 (S-F ₂), 1.550 (O-S)
SO ₂ F ₂	−2.429	−0.981		2.029		3.434 (S-F ₂), 1.727 (S-F ₁), 1.542 (O ₂ -S), 1.542 (O ₁ -S)
2SO ₂	−2.223	−0.665		2.303 (Pt-O(front SO ₂))	2.256 (Pt-O(second SO ₂))	1.498 (O ₁ -S), 1.561 (O ₂ -S), 1.565 (O ₃ -S), 1.561 (O ₄ -S)
2SOF ₂	−0.934	−0.622		2.008 (Pt-F(right SOF ₂))	3.806 (Pt-F(left SOF ₂))	1.675 (S-F ₁), 1.670 (S-F ₂), 1.460 (O-S), 3.027 (S-F ₁), 1.801 (S-F ₂), 1.503 (O-S)
2SO ₂ F ₂	−2.159	−1.088		2.009 (Pt-F(left SO ₂ F ₂))	3.422 (Pt-F(right SO ₂ F ₂))	2.343 (S-F ₁), 3.384 (S-F ₂), 1.492 (O ₁ -S), 1.486 (O ₂ -S) 1.606 (S-F ₃), 1.610 (S-F ₄), 1.441 (O ₃ -S), 1.445 (O ₄ -S)
SO ₂ &SOF ₂	−1.431	−0.321 (SO ₂)	0.127 (SOF ₂)	2.246 (Pt-O(SO ₂))	2.486 (Pt-S(SOF ₂))	1.501 (O ₁ -S), 1.589 (O ₂ -S) 1.643 (S-F ₁), 1.661 (S-F ₂), 1.455 (O-S)
SO ₂ &SO ₂ F ₂	−2.198	−0.039 (SO ₂)	−0.544 (SO ₂ F ₂)	3.983 (Pt-S(SO ₂))	2.011 (Pt-F(SO ₂ F ₂))	1.480 (O ₁ -S), 1.486 (O ₂ -S) 2.975 (S-F ₂), 1.763 (S-F ₁), 1.586 (O ₂ -S), 1.483 (O ₁ -S)
SOF ₂ &SO ₂ F ₂	−2.306	−0.047 (SOF ₂)	−0.994 (SO ₂ F ₂)	4.143 (Pt-S(SOF ₂))	2.031 (Pt-F(SO ₂ F ₂))	1.662 (S-F ₁), 1.688 (S-F ₂), 1.465 (O-S) 3.143 (S-F ₂), 1.764 (S-F ₁), 1.585 (O ₂ -S), 1.482 (O ₁ -S)

In Table 1 and Table S5 and Figure 5a–c are the adsorption parameters and adsorption structures of Pt-graphene adsorbed double hetero-gas molecules. When the mixed gas SO_2 and SOF_2 is adsorbed on Pt-graphene, the S-O bond length in the SO_2 gas molecule is extended from 1.480 Å to 1.501 Å ($\text{O}_1\text{-S}$) and 1.589 Å ($\text{O}_2\text{-S}$), respectively. Similar to the adsorption of single and double SO_2 processes in Figures 3a and 4a, the interaction of Pt-doped graphene with SO_2 gas molecules may form a new Pt-O bond that leads to the stretching of the S-O. However, the molecular structure of SOF_2 did not change, and the adsorption distance was 2.486 Å. Conversely, for the adsorption of SO_2 and SO_2F_2 mixed gas on Pt-graphene in Figure 5b, the molecular structure of SO_2 gas is unchanged, the S atom is close to the Pt metal atom, the adsorption distance is 3.983 Å, and the S-F bond length of SO_2F_2 was extended to 2.975 Å. Therefore, SO_2F_2 gas molecules breaks into a F atom and a SO_2F piece adsorbed on the Pt-graphene surface. In the case of adsorbing SOF_2 and SO_2F_2 in Figure 5c, a F atom is decomposed and adsorbed on the Pt atom. The SOF_2 molecule is far from Pt-graphene and is 4.143 Å away from the surface. The adsorption energies of the three mixed gases, SO_2 and SOF_2 , SO_2 and SO_2F_2 and SOF_2 and SO_2F_2 are -1.431 eV, -2.198 eV and -2.306 eV. The charge transfer amount Q_T of SO_2 and SO_2F_2 and SOF_2 and SO_2F_2 with Pt-doped graphene surface is $-0.039 e$, $-0.544 e$ and $-0.047 e$, $-0.994 e$ for every gas molecule. It is shown that in the adsorption process, electrons are transferred from the surface of Pt-doped graphene to gas molecules, and the gas molecules SO_2 , SOF_2 and SO_2F_2 all exhibit the characteristics of electron acceptors. The amount of charge transfer after adsorption of SO_2 and SOF_2 mixed gas is $-0.321 e$, $0.127 e$, indicating that electrons are transferred from the surface of Pt-doped graphene to SOF_2 to SO_2 gas molecules, and SO_2 is an electron acceptor but the SOF_2 is an electron donor.

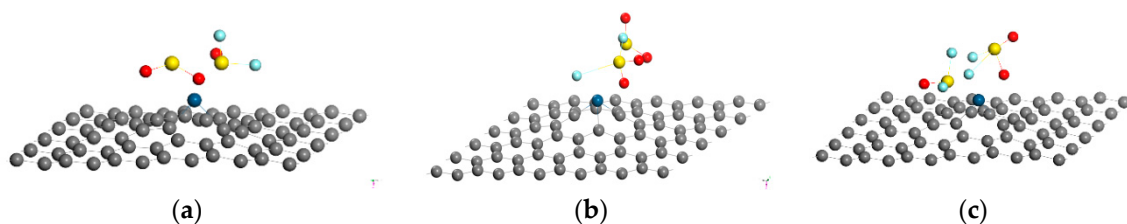


Figure 5. The adsorption structures for double foreign SO_2 , SOF_2 and SO_2F_2 adsorption on Pt-graphene. (a) SO_2 and SOF_2 ; (b) SO_2 and SO_2F_2 ; (c) SOF_2 and SO_2F_2 .

3.2.2. Analysis of Electronic Density of States

In this section, we analyze the electronic density of states (DOS) of individual gas molecules SO_2 , SOF_2 and SO_2F_2 . The DOS diagrams of Pt-graphene are shown in Figures 6–8, which confirms that the system modified by Pt atom has good conductivity. Comparing with Figure 6a, b the DOS at Fermi level increased significantly after SO_2 adsorption, which is attributed to the increase of the carrier number after SO_2 adsorption. As shown in Figure 6c, the DOS of the system adsorbed SOF_2 increases slightly below the Fermi level, but the DOS above the Fermi level is unchanged. The DOS at the Fermi level also increase. For a single SO_2F_2 adsorption (Figure 6d), DOS on the left side of Fermi level increases, but DOS on the right-side decreases, and there is no significant change at Fermi level.

In fact, the decomposition products present in the SF_6 insulating device is a mixed gas. Therefore, the adsorption of multiple gas molecules was considered in this study. Due to the limited adsorption capacity of a single Pt-doped graphene, the adsorption of two gas molecules is sufficient to analyze the adsorption of multiple gas molecules.

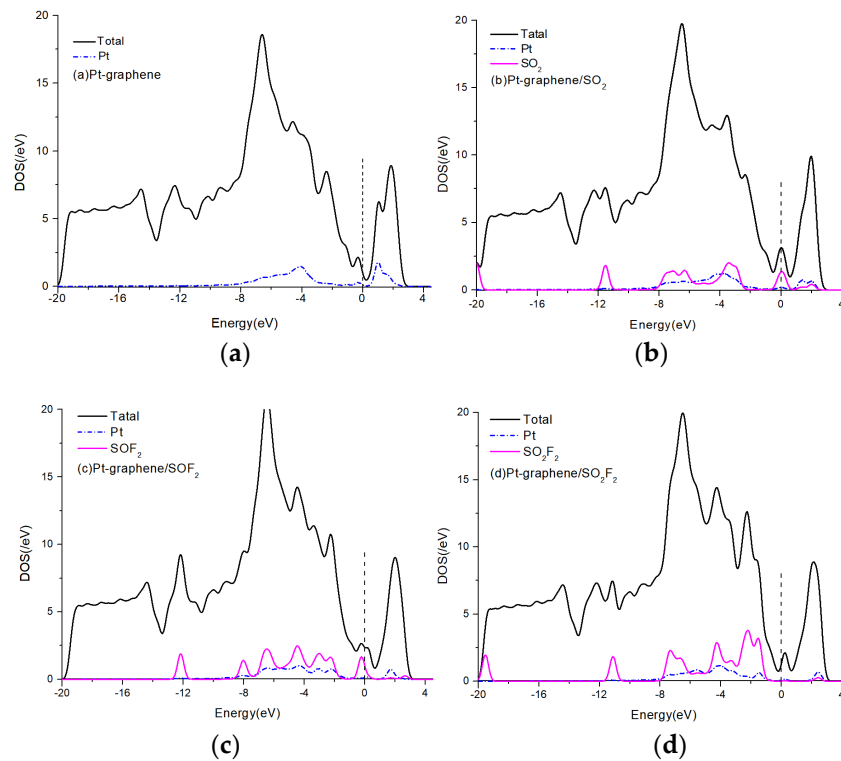


Figure 6. The change of density of states (DOS) (a) before and after (b) single SO₂, (c) single SOF₂ and (d) single SO₂F₂ adsorption on Pt-graphene.

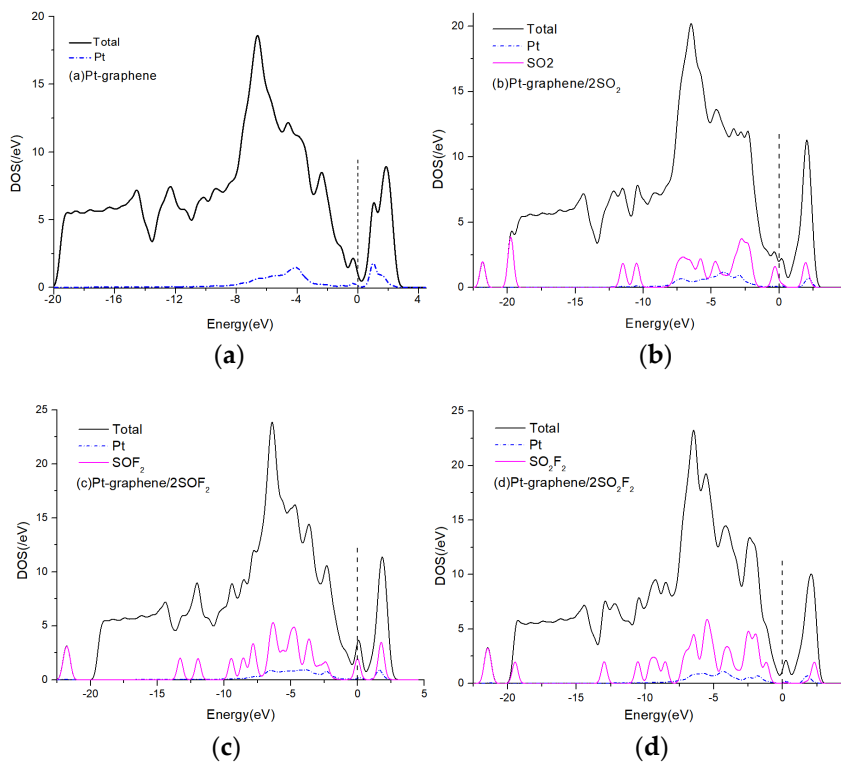


Figure 7. The change of DOS (a) before and after (b) double SO₂, (c) double SOF₂ and (d) double SO₂F₂ adsorption on Pt-graphene.

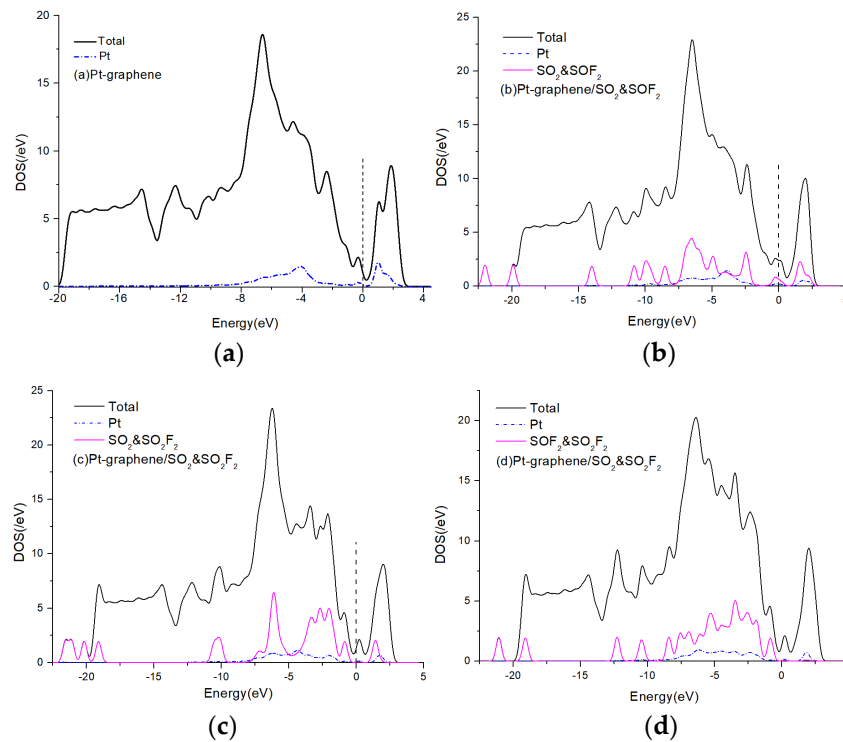


Figure 8. The change of DOS (a) before and after (b) SO_2 & SOF_2 , (c) SO_2 & SO_2F_2 and (d) SOF_2 & SO_2F_2 adsorption on Pt-graphene.

Firstly, the adsorption characteristics of adsorbed double gas molecules are discussed. The comparison of DOS before and after adsorbing gas molecules is shown in Figure 7. Two SO_2 adsorbed on Pt-graphene active sites at the same time enhances the molecular movement between Pt-graphene and adsorbing gas. Comparing with Figure 7a, b DOS has been improved in all energy distribution regions. Although the DOS curve lower than Fermi level changes little, the DOS higher than Fermi level increases. When two identical SOF_2 and SO_2F_2 molecules interact with Pt-graphene, the DOS near the Fermi level increases. As can be seen in Figure 7c, the DOS after adsorption of SOF_2 is significantly increased at the Fermi level, and as shown in Figure 7d, the DOS at the Fermi level is increased after the adsorption of SO_2F_2 .

In the case of a mixed gas decomposed in the SF_6 insulation equipment, in addition to the above-mentioned double gas adsorption, the Pt-graphene surface also adsorbs different gas molecules. According to the DOS shown in Figure 8, compared with the adsorption of single and double gas molecules, the change of DOS is significantly different, and all DOS diagrams close to the Fermi level are increased, and the overall DOS obviously moves to the right which is attributed to the change of Fermi-level compared to the bare Pt-graphene. It means that the conductivity decreases significantly. When SO_2 and SOF_2 interact with Pt-graphene, the SOF_2 molecule leaves the Pt-graphene surface according to the structure discussed above. Comparing SO_2 and SOF_2 adsorbed DOS (Figure 8b) compared with DOS single SO_2 adsorption, we found that DOS changes showed the same growth trend due to the key role of SO_2 adsorption. For the adsorption of SOF_2 and SO_2F_2 as the structure shown in Figure 8d, only the fractured fluorine atom and one SOF_2 contribute to the change of conductivity. In the process of adsorption, SO_2F_2 molecules are away from the surface of graphene, and only one F atom forms a chemical bond with Pt atoms. The increase of DOS below the Fermi level mainly comes from the contribution of F atoms adsorption.

3.2.3. Analysis of Frontier Molecular Orbital

The HOMO, LUMO and the value of E_g of the system after adsorbing a single gas molecule are shown in Table 2. It was found that E_g increased to some extent during all the adsorption processes. Before Pt-graphene adsorbed gas molecules, HOMO and LUMO were mainly distributed at Pt atoms and their opposite sides (Figure 9a). The corresponding energy gap width E_g was 0.28 eV. As shown in Figure 9b, after adsorption of SO_2 , the HOMO and LUMO were slightly transferred to the SO_2 adsorption site, and more uniformly distributed on the surface of Pt-graphene. E_g increases to 0.601 eV. We estimate that with the increase of E_g leads to the slightly decreased conductivity of the system. When a single SOF_2 molecule is adsorbed on Pt-graphene, it is not much different from the adsorption of SO_2 , and the E_g is increased to 0.667 eV. There was almost no change in HOMO. The SOF piece causes change in LUMO. For SO_2F_2 adsorption, the E_g value is 0.716 eV, and HOMO and LUMO were significantly reduced. The HOMO and LUMO adsorption configurations of Pt-graphene adsorbed SO_2F_2 are shown in Figure 9d. There are few orbits around the adsorbed SO_2F_2 .

Table 2. Highest occupied molecular orbital (HOMO), lowest unoccupied molecular orbital (LUMO), E_g before and after adsorption of single SO_2 , SOF_2 , SO_2F_2 by Pt-graphene.

System	LUMO (eV)	HOMO (eV)	E_g (eV)
Pt-graphene	−3.798	−4.229	0.489
Pt-graphene/ SO_2	−4.105	−4.706	0.601
Pt-graphene/ SOF_2	−4.218	−4.884	0.667
Pt-graphene/ SO_2F_2	−4.330	−5.046	0.716

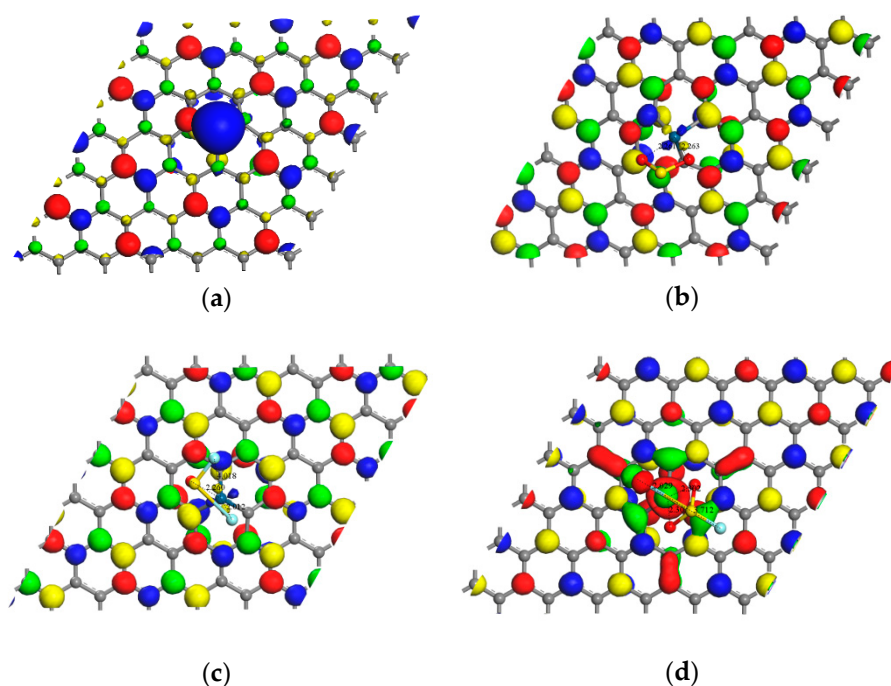


Figure 9. Distribution of HOMO (red-green) and LUMO (blue-yellow) (a) before and after (b) single SO_2 , (c) single SOF_2 and (d) single SO_2F_2 adsorption on Pt-graphene.

The HOMO, LUMO and E_g of the system after adsorption of mixed gas molecules are shown in Table 3. The HOMO and LUMO distribution (Figure 10b) has been extended to the adsorbed SO_2 and SOF_2 molecule, and the E_g is broadened to 0.564 eV. Therefore, we evaluate that the effect of SO_2 and SOF_2 adsorption slightly increases the conductivity of Pt-graphene. Although the SO_2F_2 molecule is too far away to affect the frontier molecular orbital (Figure 10c), the adsorbed SO_2 increasing the HOMO and LUMO distribution to change the system conductivity. For the HOMO and LUMO

distributions of SOF₂-SO₂F₂ adsorption shown in Figure 10d, part of the HOMO is distributed on the bonded F surface and one SOF₂ molecule, and LUMO is uniformly distributed on the C atom as compared with before adsorption. In addition, with E_g rising to 0.706 eV, HOMO and LUMO mainly distribute around F-Pt bond and SOF₂ molecule.

Table 3. HOMO, LUMO, E_g before and after adsorption of double foreign SO₂, SOF₂, SO₂F₂ by Pt-graphene.

System	LUMO	HOMO	E_g (eV)
graphene	−3.798	−4.229	0.489
Pt-graphene/SO ₂ & SOF ₂	−4.279	−4.843	0.564
Pt-graphene/SO ₂ & SO ₂ F ₂	−4.645	−5.349	0.704
Pt-graphene/SOF ₂ &SO ₂ F ₂	−4.607	−5.314	0.706

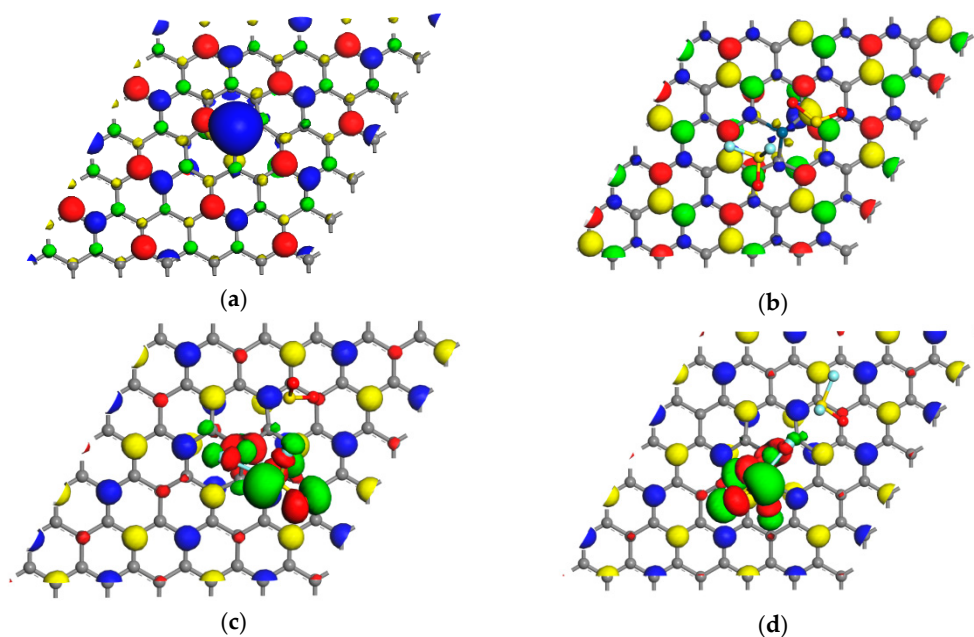


Figure 10. Distribution of HOMO (red-green) and LUMO (blue-yellow) (a) before and after (b) SO₂ & SOF₂, (c) SO₂ & SO₂F₂ and (d) SOF₂ & SO₂F₂ adsorption on Pt-graphene.

4. Conclusions

For the adsorption of a single gas molecule, Pt-doped graphene has strong interactions with SO₂, SOF₂ and SO₂F₂. For SO₂ adsorption, the energy gap width E_g decrease, which may result in the decrease of conductivity of the system. Compared with SO₂, the E_{ads} for single SOF₂ adsorption was slightly smaller, but the Q_T was slightly larger and the E_g was also slightly higher, which proved that SOF₂ brings the smallest chemical interactions but still leads to the decrease of the conductivity. The adsorption of SO₂F₂ is a strong chemisorption process and moreover, the bonds in gas molecule tend to be broken. The adsorption of SO₂F₂ also brings conductivity decrease. For the adsorption of double gas molecules, the increase in the number of molecules does not obviously change the chemical interactions to some gas molecule but may have very small interactions with the second adsorbed molecule. When adsorbing double SO₂, the adsorption energy and charge transfer amount are significantly increased compared with single gas molecules, but those of the adsorption of 2SOF₂ and 2SO₂F₂ had not change. For the adsorption of two different gas molecules, the interactions are quite different with one molecule adsorption and the conductivity decreases to varying degrees and the distribution of HOMO, LUMO orbitals transfer around the gas molecule with different degrees and the value of E_g experience different changes.

Supplementary Materials: The following are available online at <http://www.mdpi.com/2076-3417/8/10/2010/s1>, Figure S1: Adsorption structure and adsorption energy comparison of single molecule adsorbed on Pt-graphene. Figure S2: Adsorption structure and adsorption energy comparison of double SO₂, SOF₂ and SO₂F₂ adsorbed on Pt-graphene. Figure S3: Adsorption structure and adsorption energy comparison of double double foreign molecules adsorbed on Pt-graphene. Table S1: Cartesian coordinates of SO₂, SOF₂ and SO₂F₂. Table S2: Cartesian coordinates of graphene and Pt-graphene. Table S3: Cartesian coordinates of single molecule adsorbed on Pt-graphene. Table S4: Cartesian coordinates of double molecule (2SO₂, 2SOF₂, 2SO₂F₂) adsorbed on Pt-graphene. Table S5: Cartesian coordinates of double molecule (SO₂& SOF₂, SO₂& SO₂F₂, SOF₂& SO₂F₂) adsorbed on Pt-graphene

Author Contributions: S.S. and X.Z. proposed the project and revised the manuscript. Y.W. and D.C. contributed to the theoretical simulation and analyzed the simulation results. All authors read and approved the final manuscript.

Funding: The authors are very grateful to the support by the Natural Science Foundation of the Guangxi Province (No. 2016GXNSFAA380327). This work is also supported by the National Natural Science Foundation of China under Grant 51777144.

Conflicts of Interest: The authors declare no conflict of interest.

References

1. Chu, F.Y. SF₆ decomposition in gas-insulated equipment. *IEEE Trans. Electr. Insul.* **1986**, *EI-21*, 693–725. [[CrossRef](#)]
2. Xie, Q.; Cheng, S.; Lü, F.; Li, Y. Location of partial discharge in transformer oil using circular array of ultrasonic sensors. *IEEE Trans. Dielectr. Electr. Insul.* **2013**, *20*, 1683–1690. [[CrossRef](#)]
3. Liu, Y.W.; Wu, L.Y.; Gong, Y.P. Investigation on SF₆ Decomposition Products in GIS and Affecting Factors. *Power Syst. Technol.* **2009**, *5*, 015.
4. Okabe, S.; Kaneko, S.; Minagawa, T.; Nishida, C. Detecting characteristics of SF₆ decomposed gas sensor for insulation diagnosis on gas insulated switchgears. *IEEE Trans. Dielectr. Electr. Insul.* **2008**, *15*, 251–258. [[CrossRef](#)]
5. Tang, J.; Liu, F.; Zhang, X.; Meng, Q.; Zhou, J. Partial discharge recognition through an analysis of SF₆ decomposition products part 1: Decomposition characteristics of SF₆ under four different partial discharges. *IEEE Trans. Dielectr. Electr. Insul.* **2012**, *19*, 29–36. [[CrossRef](#)]
6. Tang, J.; Liu, F.; Meng, Q.; Zhang, X.; Tao, J. Partial discharge recognition through an analysis of SF₆ decomposition products part 2: Feature extraction and decision tree-based pattern recognition. *IEEE Trans. Dielectr. Electr. Insul.* **2012**, *19*, 37–44. [[CrossRef](#)]
7. Sun, P.; Wang, K.; Zhu, H. Recent Developments in Graphene-Based Membranes: Structure, Mass-Transport Mechanism and Potential Applications. *Adv. Mater.* **2016**, *28*, 2287–2310. [[CrossRef](#)] [[PubMed](#)]
8. Huang, X.; Yin, Z.; Wu, S.; Qi, X.; He, Q.; Zhang, Q.; Zhang, H. Graphene-based materials: Synthesis, characterization, properties, and applications. *Small* **2011**, *7*, 1876–1902. [[CrossRef](#)] [[PubMed](#)]
9. Zhang, H.; Li, F.; Liu, K. Research Progress in Gas Sensitivity of Graphene. *Mater. Rev.* **2012**, *S2*, 39–43.
10. Schedin, F.; Geim, A.K.; Morozov, S.V.; Hill, E.W.; Blake, P.; Katsnelson, M.I.; Novoselov, K.S. Detection of individual gas molecules adsorbed on graphene. *Nat. Mater.* **2007**, *6*, 652–655. [[CrossRef](#)] [[PubMed](#)]
11. Chu, J.; Wang, X.; Wang, D.; Yang, A.; Lv, P.; Wu, Y.; Rong, M.; Gao, L. Highly selective detection of sulfur hexafluoride decomposition components H₂S and SOF₂ employing sensors based on tin oxide modified reduced graphene oxide. *Carbon* **2018**, *135*, 95–103. [[CrossRef](#)]
12. Zhang, Y.H.; Chen, Y.B.; Zhou, K.G.; Liu, C.H.; Zeng, J.; Zhang, H.L.; Peng, Y. Improving gas sensing properties of graphene by introducing dopants and defects: A first-principles study. *Nanotechnology* **2009**, *20*, 185504. [[CrossRef](#)] [[PubMed](#)]
13. Beheshtian, J.; Peyghan, A.A.; Noei, M. Sensing behavior of Al and Si doped BC₃ graphenes to formaldehyde. *Sens. Actuators B Chem.* **2013**, *181*, 829–834. [[CrossRef](#)]
14. Xiao, H.; Shi, X.; Zhang, Y.; Li, M.; Liao, X.; Chen, X. Predicting a two-dimensional P₂S₃ monolayer: A global minimum structure. *Comput. Mater. Sci.* **2018**, *155*, 288–292. [[CrossRef](#)]
15. Xiao, H.; Shi, X.; Liao, X.; Zhang, Y.; Chen, X. Prediction of a two-dimensional S₃N₂ solid for optoelectronic applications. *Phys. Rev. Mater.* **2018**, *2*, 024002. [[CrossRef](#)]
16. Leenaerts, O.; Partoens, B.; Peeters, F.M. Adsorption of H₂O, NH₃, CO, NO₂, and NO on graphene: A first-principles study. *Phys. Rev. B* **2008**, *77*, 125416. [[CrossRef](#)]

17. Tang, Y.; Liu, Z.; Shen, Z.; Chen, W.; Ma, D.; Dai, X. Adsorption sensitivity of metal atom decorated bilayer graphene toward toxic gas molecules (CO, NO, SO₂ and HCN). *Sens. Actuators B Chem.* **2017**, *238*, 182–195. [[CrossRef](#)]
18. Shokuhi Rad, A. DFT study of nitrous oxide adsorption on the surface of Pt-decorated graphene. *Phys. Chem. Res.* **2016**, *4*, 619–626.
19. Rad, A.S.; Abedini, E. Chemisorption of NO on Pt-decorated graphene as modified nanostructure media: A first principles study. *Appl. Surf. Sci.* **2016**, *360*, 1041–1046. [[CrossRef](#)]
20. Rad, A.S. Adsorption of C₂H₂ and C₂H₄ on Pt-decorated graphene nanostructure: Ab-initio study. *Synth. Met.* **2016**, *211*, 115–120. [[CrossRef](#)]
21. Rad, A.S. Density functional theory study of the adsorption of MeOH and EtOH on the surface of Pt-decorated graphene. *Phys. E Low-Dimens. Syst. Nanostruct.* **2016**, *83*, 135–140. [[CrossRef](#)]
22. Rad, A.S.; Zareyee, D. Adsorption properties of SO₂ and O₃ molecules on Pt-decorated graphene: A theoretical study. *Vacuum* **2016**, *130*, 113–118.
23. Chen, D.; Zhang, X.; Tang, J.; Fang, J.; Li, Y.; Liu, H. Adsorption and dissociation mechanism of SO₂ and H₂S on Pt decorated graphene: A DFT-D3 study. *Appl. Phys. A* **2018**, *124*, 404. [[CrossRef](#)]
24. Delley, B. An all-electron numerical method for solving the local density functional for polyatomic molecules. *J. Chem. Phys.* **1990**, *92*, 508–517. [[CrossRef](#)]
25. Delley, B. From molecules to solids with the DMol3 approach. *J. Chem. Phys.* **2000**, *113*, 7756–7764. [[CrossRef](#)]
26. Perdew, J.P.; Burke, K.; Ernzerhof, M. Generalized gradient approximation made simple. *Phys. Rev. Lett.* **1996**, *77*, 3865. [[CrossRef](#)] [[PubMed](#)]
27. Grimme, S. Semiempirical GGA-type density functional constructed with a long-range dispersion correction. *J. Comput. Chem.* **2006**, *27*, 1787–1799. [[CrossRef](#)] [[PubMed](#)]
28. Monkhorst, H.J.; Pack, J.D. Special points for Brillouin-zone integrations. *Phys. Rev. B* **1976**, *13*, 5188. [[CrossRef](#)]
29. Mulliken, R.S. Electronic population analysis on LCAO–MO molecular wave functions. I. *J. Chem. Phys.* **1955**, *23*, 1833–1840. [[CrossRef](#)]
30. Fu, Y.; Yang, A.; Wang, X.; Murphy, A.B.; Li, X.; Liu, D.; Wu, Y.; Rong, M. Theoretical study of the neutral decomposition of SF₆ in the presence of H₂O and O₂ in discharges in power equipment. *J. Phys. D Appl. Phys.* **2016**, *49*, 385203. [[CrossRef](#)]
31. Zhang, X.; Yu, L.; Gui, Y.; Hu, W. First-principles study of SF₆ decomposed gas adsorbed on Au-decorated graphene. *Appl. Surf. Sci.* **2016**, *367*, 259–269. [[CrossRef](#)]
32. Del Castillo, R.M.; Sansores, L.E. Study of the electronic structure of Ag, Au, Pt and Pd clusters adsorption on graphene and their effect on conductivity. *Eur. Phys. J. B* **2015**, *88*, 248. [[CrossRef](#)]

